



HAL
open science

Aqueous chemistry of Ce(IV): estimations using actinide analogues

Rémi M Marsac, Florent Réal, Nidhul Lal Banik, Mathieu Pédrot, Olivier Pourret, Valérie Vallet

► **To cite this version:**

Rémi M Marsac, Florent Réal, Nidhul Lal Banik, Mathieu Pédrot, Olivier Pourret, et al.. Aqueous chemistry of Ce(IV): estimations using actinide analogues. Dalton Transactions, 2017, 46 (39), pp.13553-13561. 10.1039/C7DT02251D . insu-01588240

HAL Id: insu-01588240

<https://insu.hal.science/insu-01588240>

Submitted on 15 Sep 2017

HAL is a multi-disciplinary open access archive for the deposit and dissemination of scientific research documents, whether they are published or not. The documents may come from teaching and research institutions in France or abroad, or from public or private research centers.

L'archive ouverte pluridisciplinaire **HAL**, est destinée au dépôt et à la diffusion de documents scientifiques de niveau recherche, publiés ou non, émanant des établissements d'enseignement et de recherche français ou étrangers, des laboratoires publics ou privés.

1 **Aqueous chemistry of Ce(IV): estimations using actinide analogues**

2

3 Rémi Marsac^{a*}, Florent Réal^b, Nidhu Lal Banik^c, Mathieu Pédrot^a, Olivier Pourret^d, Valérie
4 Vallet^b

5

6

7 ^aGéosciences Rennes UMR 6118, Université Rennes 1, CNRS, 35042 Rennes cedex, France

8 ^bUniv. Lille, CNRS, UMR 8523 – PhLAM – Physique des Lasers Atomes et Molécules, F-59000
9 Lille, France

10 ^cJRC-KARLSRUHE, G.II.6 - Nuclear Safeguards and Forensics, European Commission, P.O.Box
11 2340, D-76125 Karlsruhe, Germany

12 ^dHydrISE, UniLaSalle, 60026 Beauvais cedex, France

13

14 *Corresponding author : Géosciences Rennes UMR 6118, Université Rennes 1, CNRS, 35042
15 Rennes cedex, France. E-mail address: remi.marsac@univ-rennes1.fr (R. Marsac).

16

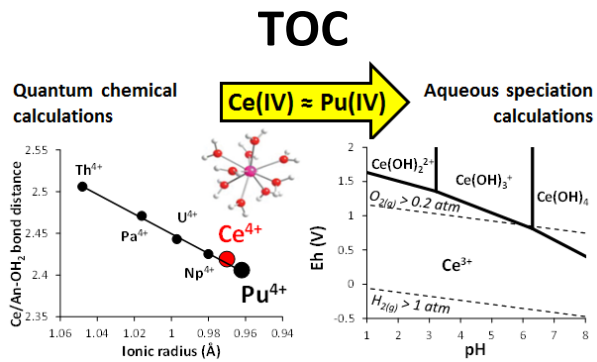
17 **Abstract**

18 Prediction of Cerium (Ce) aqueous speciation is relevant in many research fields. Indeed, Ce
19 compounds are used for many industrial applications, which may require the control of Ce aqueous
20 chemistry for their synthesis. Aquatic geochemistry of Ce is also of interest. Due to growing
21 industrial use and its release to the environment, Ce is now considered as emerging contaminant.
22 Cerium is also used as a proxy of (paleo)redox conditions due to the Ce(IV)/Ce(III) redox
23 transition. Finally, Ce(IV) is often presented as a relevant analogue of tetravalent actinides
24 (An(IV)). In the present study, quantum chemical calculations were conducted to highlight
25 similarities between the structure of Ce(IV) and tetravalent actinides (An(IV); An = Th, Pa, U, Np,
26 Pu) aqua-ions, especially Pu(IV). Current knowledge of An(IV) hydrolysis, solubility and colloid
27 formation in water were briefly reviewed but important discrepancies observed with available data
28 for Ce(IV). Therefore, new estimation of the hydrolysis constants of Ce(IV) and solubility of
29 Ce(IV)-(hydr)oxides are proposed, by analogy with Pu(IV). By plotting pH-Eh (Pourbaix)
30 diagrams, we showed that the pH values corresponding to the onset of Ce(IV) species formation
31 (i.e. Ce(IV)-(hydr)oxide or dissolved Ce(IV)) agreed with various experimental results. Although,
32 further experimental studies are required to obtain a more accurate thermodynamic database, the
33 present work might yet help to predict more accurately Ce chemical behavior in aqueous solution.

34 **Keywords:** Cerium, actinide, tetravalent, hydrolysis, solubility, speciation, aqua-ions, quantum
35 chemical calculation.

36

37



38

39 Quantum chemical calculations and a comparison of Cerium(IV)/Actinide(IV) justify the
40 estimation of Cerium(IV) aqueous speciation using Plutonium(IV) as analogue.

41

42 **Introduction**

43 The solution chemistry of actinide (An) ions in aquatic systems relevant for the disposal of
44 nuclear wastes is influenced by hydrolysis reactions and complexation with inorganic and organic
45 anions.¹ Actinides can be found in various oxidation states in aqueous solution, which commonly
46 range from +III to +VI depending on the An (i.e., Th, U, Np, Pu). Change in oxidation state has
47 drastic consequences on An aqueous chemistry, solubility and sorption to natural organic and
48 inorganic particles and colloids, which, in turn, affect their mobility in natural systems.²⁻⁹ Only
49 Th(IV) exists in aqueous solution. U(IV) and U(VI) prevail in reducing and oxidizing conditions,
50 respectively, the stability field of U(V) (found in moderately reducing conditions) being rather
51 narrow.¹⁰ Np(IV) and Np(V) are the prevalent oxidation states of Np but Np(VI) can form in
52 oxidizing alkaline solutions.^{8,11,12} Pu can be found in oxidation states ranging from +III to +VI in
53 environmentally relevant conditions.^{3,7,13} For all these An elements, the tetravalent oxidation state
54 is pertinent in near-neutral pH values expected to be found in nature. Because of their high electric
55 charge, tetravalent actinide ions have a strong tendency toward hydrolysis in aqueous solution and
56 undergo polynucleation or further lead to colloid formation.¹⁴ Therefore, many studies were
57 dedicated to An(IV) hydrolysis, solubility and colloids formation.¹⁵⁻¹⁹ The chemical behavior of
58 An(IV) was found highly consistent across the series, as commonly observed for f-elements
59 (lanthanides (Ln) (4f) and An (5f)) in the same oxidation state, and are thus often considered as
60 chemical analogues (e.g.²⁰⁻²⁵).

61 Lanthanides are naturally occurring trace elements in the environment. In contrast to its
62 lanthanide neighbors, which predominate in +III oxidation state, Ce(III) can be oxidized to Ce(IV)
63 under oxidizing conditions. Preferential removal of Ce(IV) than Ce(III) from aqueous solution by
64 natural particles can lead to the development of a so-called Ce anomaly (implicitly, by comparison

65 with the behavior of its lanthanide neighbors La(III) and Pr(III)). The presence (under oxidizing
66 conditions) or the absence (under more reducing conditions) of a Ce anomaly in natural samples is
67 widely used as a proxy of (paleo)redox conditions.^{26–29} Since Ce is also used for many
68 applications,^{30–34} it is now considered as emerging contaminant that could affect ecosystems, due
69 to its release to the environment.³⁰ Ce(IV) is often presented as a relevant analogue of
70 An(IV).^{22,24,25} As Ce is not radioactive, experimental studies can be more easily conducted with
71 Ce(IV) than with An(IV), which could improve our scientific knowledge on An(IV) environmental
72 chemistry. Therefore, prediction of Ce aqueous speciation is of great interest for different research
73 fields.

74 However, by contrast with An(IV), there is much less information regarding Ce(IV)
75 aqueous chemistry. In fact, the present situation is such that it might be more appropriate to use
76 An(IV) to shed light on Ce(IV) aqueous chemistry than the contrary. For instance, thermodynamic
77 constants selected by Baes and Mesmer³⁵ are often used to predict Ce(IV) hydrolysis and solubility
78 in water. This database only contains formation constants for $\text{CeOH}^{3+}_{(\text{aq})}$ and $\text{Ce}(\text{OH})_2^{2+}_{(\text{aq})}$, and is
79 obviously incomplete because at least the electrically neutral $\text{Ce}(\text{OH})_{4(\text{aq})}$ species should be in
80 equilibrium with Ce(IV)-(hydr)oxides at neutral and/or alkaline pH. Omission of such species
81 inevitably leads to drastic underestimation of Ce(IV) solubility. Hayes et al.³⁶ used hydrolysis
82 constants of Ce(IV) more recently determined by Bilal and Müller³⁷ to plot a pH-Eh predominance
83 diagram. According to these results, under ambient conditions (air; $P_{\text{O}_2} = 0.2$ atm), Ce(IV) should
84 prevail at pH above ~4.5. This result contrasts with Th(IV) and lanthanide adsorption studies on
85 $\text{MnO}_{2(\text{s})}$ which is known to rapidly oxidize Ce(III) to Ce(IV). Almost complete and
86 pH-independent uptake of Th(IV) by $\text{MnO}_{2(\text{s})}$ is observed for $3 < \text{pH} < 11$.³⁸ By contrast, although
87 more efficiently removed from the solution by $\text{MnO}_{2(\text{s})}$ than its lanthanide neighbors, only partial

88 uptake of Ce (initially +III) by $\text{MnO}_{2(s)}$ is observed under ambient air and it increases from pH = 4
89 to pH = 6-7.^{29,39} This suggests that, at $4 < \text{pH} < 6-7$, although Ce(IV) is associated with the solid
90 phase (precipitated or adsorbed on $\text{MnO}_{2(s)}$), Ce(III) prevails in solution,⁴⁰ as also observed in
91 previous studies dealing with Pu uptake by clays in moderately reducing conditions (where the
92 Pu(IV)/Pu(III) redox couple was involved).^{41,42} Therefore, Ce(IV) hydrolysis constants determined
93 by Bilal and Müller³⁷ appear to be questionable.

94 In this study, we briefly summarized current knowledge about An(IV) aqua-ions structure,
95 hydrolysis, solubility and colloids formation in water, in the absence of complexing ligands.
96 Quantum chemical calculations were conducted to highlight similarities between the structure of
97 Ce(IV) and Th/U/Np/Pu(IV) aqua-ions. Because available hydrolysis constants and solubility data
98 for Ce(IV) were found partly inconsistent with those of Th/U/Np/Pu(IV), new estimated
99 thermodynamic constants for Ce(IV) were proposed.

100

101 **Materials and methods**

102 **Quantum chemical calculations**

103 The quantum chemical methodology used to discuss the structure and relative free energies of
104 Ce(IV) hydrates with 10, 9 and 8 water molecules $[\text{Ce}(\text{H}_2\text{O})_{10}]^{4+}$, $[\text{Ce}(\text{H}_2\text{O})_9]^{4+} \cdot \text{H}_2\text{O}$, and
105 $[\text{Ce}(\text{H}_2\text{O})_8]^{4+} \cdot (\text{H}_2\text{O})_2$ is similar to that of our previous study on early tetravalent An species.⁴³ A
106 small-core relativistic effective core potential⁴⁴ of the Stuttgart-Cologne group was employed for
107 the cerium atom along with the corresponding segmented basis set.⁴⁵ Augmented
108 correlation-consistent polarization valence triple- ζ (aug-cc-pVTZ) basis sets were used for
109 oxygen,⁴⁶ and hydrogen atoms.⁴⁷ The geometries were optimized without symmetry constraints at

110 the restricted MP2 level using the parallel resolution of the identity approximation,^{48,49} with the
111 appropriate atomic auxiliary basis functions.^{50,51} Harmonic frequency calculations were computed
112 numerically at the optimized geometry, not only to confirm that the optima found correspond to
113 energy minima, but also to compute the vibrational partition functions at 298.15 K and 0.1 MPa,
114 which are necessary to calculate the enthalpic and entropic contributions to the gas-phase energies.
115 The contribution of hydration to the free energies of all isomers was estimated by single-point
116 COSMO calculations with a dielectric constant of 78.9.⁵² To comply with the relatively low level
117 of theory (HF or DFT with small basis sets) at which the COSMO model has been parameterized,⁵³
118 a B3LYP based density and small def2-SVP basis sets⁵⁴ on all atoms are used to compute free
119 energies of solvation. All calculations were performed with the Turbomole 7.1 quantum chemistry
120 package.⁵⁵ A comparison of the nature of the cerium-water bond with that of the other tetravalent
121 actinide elements was performed using the quantum theory of atoms in molecules (QTAIM)
122 approach, implemented in the AIMAll package,⁵⁶ that analyzes the appropriate wave function
123 extended files (wfx) obtained with Gaussian09.⁵⁷

124

125 **Geochemical speciation code and thermodynamic database**

126 PHREEQC (version 2)⁵⁸ is a computer code that can perform speciation and
127 saturation-index calculations in water. PHREEQC was used to calculate species distribution plots.
128 Predominance (pH-Eh) diagrams were obtained using PhreePlot,⁵⁹ which contains an embedded
129 version of PHREEQC. The specific ion interaction theory (SIT⁶⁰) was used to extrapolate
130 thermodynamic constants at various ionic strengths. In the present work, thermodynamic constants
131 for An aqueous speciation and solubility and SIT parameters were taken from the NEA

132 thermodynamic database². The metastability of ClO_4^- , sometimes used as background anion, is
133 avoided in the models by defining perchlorate as a master species.

134 **Results and discussion**

135 **Tetravalent actinides and cerium aqua-ions**

136 Figure 1a plots the mean An–OH₂ bond distances of tetravalent actinide aqua ions determined by
137 L₃-edge extended X-ray absorption fine structure (EXAFS) versus their ionic radii for coordination
138 number of eight.^{43,61} In a previous work, a linear relationship with a slope of about one was
139 observed for the ions from Th⁴⁺ to Pu⁴⁺.⁴³ Because the An–OH₂ bond distances for the ions up to
140 Pu⁴⁺ follow closely this line, and hence the actinide contraction, it was assumed that there is no
141 major change in these ions' hydration number. To obtain detailed information on the preferred
142 coordination structure for An⁴⁺ ions in solution quantum chemical calculations were performed on
143 the decahydrates [An(H₂O)₁₀]⁴⁺, [An(H₂O)₉]⁴⁺·H₂O, and [An(H₂O)₈]⁴⁺·(H₂O)₂ (see Fig. 1b; Table
144 S1 and S2).⁴³ Calculation of relative free energies (Table S2) showed that the nine-coordinate
145 isomer, having distorted tricapped trigonal prismatic first shell geometry, was the most stable
146 species for all ions from Th⁴⁺ to Pu⁴⁺. Although overestimated (see discussion in Vallet et al.⁶²),
147 calculated An–OH₂ bond distances follow a linear relationship with the ionic radii, as observed by
148 EXAFS.

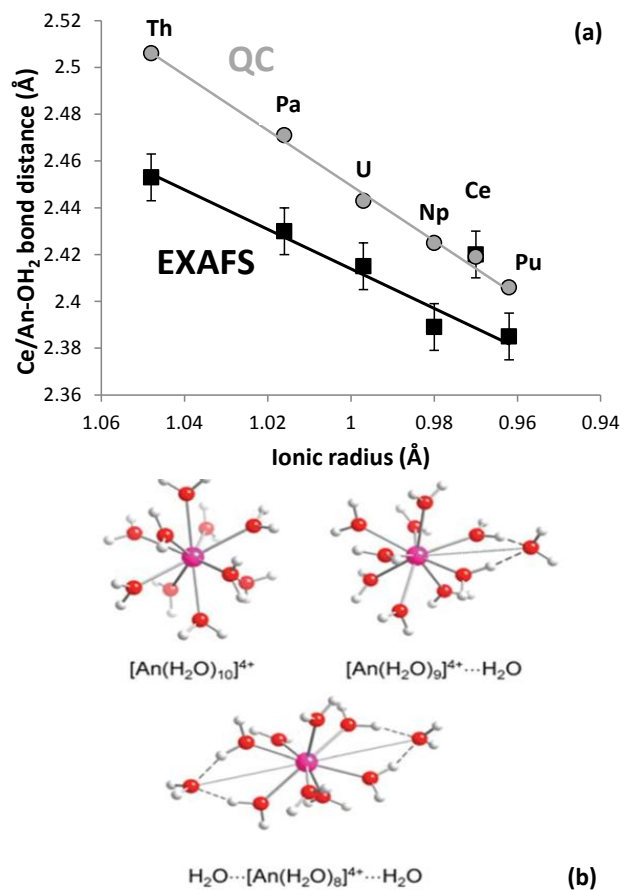
149 With an ionic radius of 0.97 Å, Ce⁴⁺ is expected to be an analogue of either Np⁴⁺ (0.98 Å) or
150 Pu⁴⁺ (0.96 Å).⁶¹ Available EXAFS data somehow disagree with this hypothesis (Figure 1a),⁶³
151 Ce⁴⁺–OH₂ bond distance (= 2.42 Å) being larger than that of Np⁴⁺ and Pu⁴⁺, but comparable to
152 Pa⁴⁺–/U⁴⁺–OH₂ bond distance (Fig. 1a; see also Table S3 of reference 43). In fact, standard redox
153 potential of Ce⁴⁺/Ce³⁺ ($E_{\text{Ce}^{4+}/\text{Ce}^{3+}}$) is larger than that of O₂/H₂O,^{36,37} hence Ce⁴⁺ is not

154 thermodynamically stable in water at acidic pH. As observed by Sham,⁶³ the solution contained a
155 mixture of Ce⁴⁺ and Ce³⁺ and the Ce⁴⁺-OH₂ bond distance was only estimated, hence subjected to
156 relatively large uncertainty. By contrast, present quantum chemical calculations confirm that, for
157 aqua-ions, (i) Ce⁴⁺ coordination number is 9 like in the early An⁴⁺, (ii) relative free energies for the
158 ten- and eight-coordinate isomers of Ce⁴⁺ are comparable to that of Np⁴⁺ and Pu⁴⁺ (Table S2) and
159 (iii) bond distance follow Np⁴⁺-OH₂ < Ce⁴⁺-OH₂ < Pu⁴⁺-OH₂ (Figure 1a). The topological
160 analysis of the electron charge density at the Ce/An⁴⁺-OH₂ bond critical points, presented in Table
161 S3, reveal that the values of all bonding indicators, the density ρ , its Laplacian $\nabla^2\rho$, the energy
162 density H_b , and the bonding index $D(M,L)$ of Ce superimpose with that of Np and Pu. This further
163 supports the strong resemblance of Ce with Np and Pu, and suggests that, as in tetravalent actinide
164 aqua ion, Ce(IV)-water bonds can be described as electrostatic. Furthermore, the difference from
165 the formal atomic valence f population in [Ce(H₂O)₉,(H₂O)]⁴⁺ are very similar to that of the Pu(IV)
166 homologue. The valence d orbitals are however, slightly more populated, simply reflecting the fact
167 the 5d states/orbitals are more energetically accessible in Ce(IV) than the 6d ones in the heavy
168 actinide (Np or Pu) homologues. To stress further the similarity between Ce(IV) and Pu(IV) ions, it
169 is worthy to mention a previous theoretical study, where the objective was to find a surrogate for
170 the Pu(IV) ion in HNO₃/TBP solution when it is complexed by nitrate ions, i.e Pu(NO₃)₆²⁻ and
171 Pu(NO₃)₄(TBP)₂.²⁴ It was found that the Ce(IV) complexes have comparable behaviors in term of
172 structures, charge distribution and stabilities to those of Pu(IV), and that Ce(IV) is *a priori* a better
173 surrogate for Pu(IV) for experimental studies than Th(IV) or U(IV). This conclusion is in line with
174 the observed applicability of cerium dioxide CeO₂ as a surrogate for plutonium dioxide PuO₂
175 steaming from their structural similarities and comparable redox behavior.⁶⁴⁻⁶⁷

176

177

178



179

180 **Figure 1.** (a) Mean An–OH₂ or Ce–OH₂ bond distance determined by L₃-edge extended X-ray absorption fine
 181 structure (EXAFS) or by quantum chemical calculations (QC; for [An/Ce(H₂O)₉]⁴⁺·H₂O) versus An/Ce(IV) ionic radii
 182 (b) (U)-MP2 gas-phase optimized isomeric 10-, 9-, and 8-coordinated clusters, [An(H₂O)₁₀]⁴⁺, [An(H₂O)₉]⁴⁺·H₂O, and
 183 [An(H₂O)₈]⁴⁺·(H₂O)₂.⁴³

184

185 **Solubility of Actinide(IV)- and Cerium(IV)-(hydr)oxides**

186 Solubility products K_{sp}^0 (at infinite dilution) of amorphous An(IV) precipitates
187 ($\text{An}(\text{OH})_{4(\text{am})}$ or $\text{AnO}\cdot x\text{H}_2\text{O}_{(\text{am})}$) and crystalline dioxides $\text{AnO}_{2(\text{cr})}$ globally refer to the dissolution
188 equilibrium:¹⁴



190 A relationships between $\log K_{sp}^0$ of $\text{An}(\text{OH})_{4(\text{am})}$ or $\text{AnO}_{2(\text{cr})}$ and the ionic radii of An^{4+} was
191 evidenced.¹⁸ Baes and Mesmer³⁵ determined $\log K_{sp}^0$ of $\text{CeO}_{2(\text{cr})}$ from data given in the NBS
192 tables,⁶⁸ which we find in excellent agreement with An(IV) (Figure 2a).

193 As previously demonstrated, the thermodynamically stable crystalline dioxides $\text{AnO}_{2(\text{cr})}$
194 may be the solubility limiting solid phase at very low pH or elevated temperature.^{14,18,19} However,
195 experimental solubility data in neutral and alkaline solutions at room temperature are 6–7 orders of
196 magnitude higher than the low values of less than 10^{-15} mol L⁻¹ calculated from the known
197 thermodynamic data. In fact, they correspond to solubility data obtained for $\text{An}(\text{OH})_{4(\text{am})}$. It was
198 concluded that hydration of the surface of crystalline $\text{AnO}_{2(\text{cr})}$ results in an amorphous solubility
199 limiting surface layer.^{14,18} By analogy with An(IV), Ce(IV) solubility might be strongly
200 underestimated in near neutral to alkaline solutions when using $\log K_{sp}^0$ of $\text{CeO}_{2(\text{cr})}$. It might be
201 more realistic to consider $\text{Ce}(\text{OH})_{4(\text{am})}$ as the solubility limiting phase.

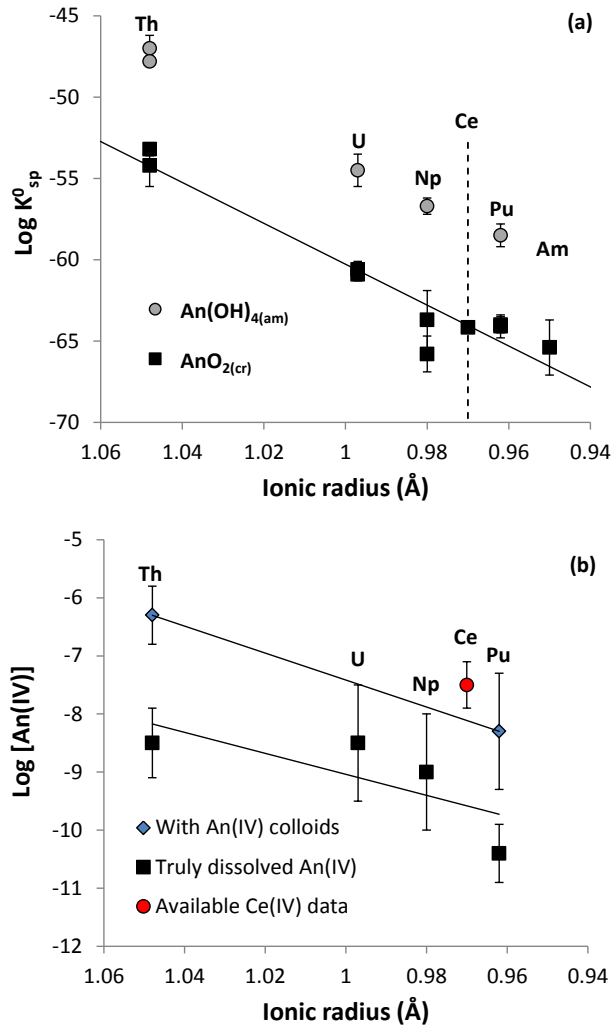
202 Actinide(IV) solubility determined in neutral and alkaline solutions by ultracentrifugation
203 (e.g. 5×10^5 g during 1h)¹⁹ or ultrafiltration (typically 10 kDa)¹⁵ refer to “truly dissolved” An(IV)
204 ($[\text{An}(\text{IV})]_{\text{aq}}$) and can be ascribed to the following solubility equilibrium:



206 Figure 2b shows that experimental values of $\log [\text{An(IV)}]_{\text{aq}}$ tend to decrease with the An(IV) ionic
207 radii. When no or insufficient phase separation is applied, the measured Th(IV) and Pu(IV)
208 concentrations in the aqueous phase are generally ~ 2.5 orders of magnitude larger.^{15,19} This was
209 attributed to the formation of small An(IV) eigencolloids. Their size was estimated to be in the
210 range 1.5–2 nm, whereas $\text{An(OH)}_{4(\text{am})}$ particles would be 2–5 nm large.¹⁵ Experimentally
211 determined apparent Th(IV) and Pu(IV) solubilities in neutral and alkaline solutions in presence of
212 eigencolloids ($[\text{An(IV)}]_{\text{coll}}$) are plotted in Figure 2b. A similar trend is found for $\log [\text{An(IV)}]_{\text{coll}}$
213 and $\log [\text{An(IV)}]_{\text{aq}}$ versus ionic radii. Although data are missing for U and Np, this result further
214 highlights the coherence across the An(IV) series.

215 Recently, the solubility of nanocrystalline cerium dioxide ($\text{CeO}_{2(\text{cr,nano})}$) was determined.⁶⁹
216 At $\text{pH} > 6$, $\log [\text{Ce(IV)}] = -7.5 \pm 0.4 (1\sigma)$ was found. This result is highly contrasting with \log
217 $[\text{An(IV)}]_{\text{aq}}$ (Fig. 2b). However, the authors performed phase separation by ultracentrifugation
218 during 4 h at $4 \times 10^4 \text{g}$. By analogy with An(IV), if we assume that Ce(IV) eigencolloids might form,
219 this set-up might be inappropriate to remove such colloids. This hypothesis is supported by the fact
220 that $\log [\text{Ce(IV)}]$ measured by Plakhova et al.⁶⁹ is in excellent agreement with $\log [\text{An(IV)}]_{\text{coll}}$ (Fig.
221 2b).

222



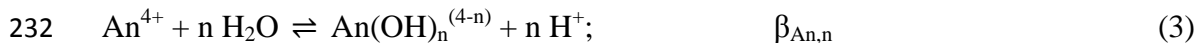
223

224 **Figure 2.** (a) Solubility products of $\text{An(OH)}_{4(\text{am})}$ and $\text{AnO}_{2(\text{cr})}$ as a function of ionic radius.¹⁸ Available data for $\text{CeO}_{2(\text{cr})}$
 225 are also included.³⁵ (b) Measured log [An(IV)] versus ionic radii at neutral to alkaline pH in equilibrium with
 226 $\text{An(OH)}_{4(\text{am})}$ after ultrafiltration or ultracentrifugation (“truly dissolved An(IV)”) and with insufficient or without
 227 phase separation (“with An(IV) colloids”).¹⁴ Value of log [Ce(IV)] determined by Plakhova et al.⁶⁹ at pH > 6 is shown
 228 for comparison.

229

230 **Hydrolysis and polynuclear species of Actinide(IV) and Cerium(IV)**

231 Actinide(IV) hydrolysis reactions can be written as follows:

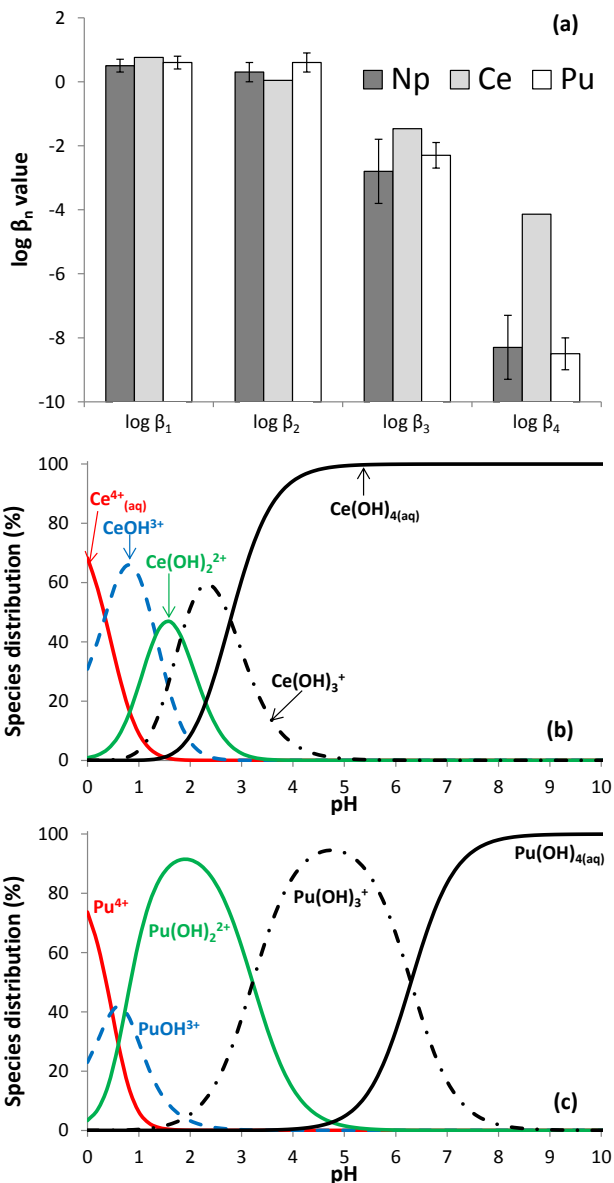


233 Where $\beta_{\text{An},n}$ is the corresponding hydrolysis constant (at infinite dilution) and $1 \leq n \leq 4$. There is no
234 evidence for the formation of $\text{An}(\text{OH})_5^-$ (aq). As reviewed by Neck et al.¹⁴ values of $\log \beta_{\text{An},n}$ are
235 consistent in the An(IV) series, and increase from Th(IV) to Pu(IV). An(IV) also tend to form
236 polynuclear species, observed for pH-[An(IV)] values approaching the solubility limit of An(IV)
237 with respect to $\text{An}(\text{OH})_{4(\text{am})}$. Polynuclear species formation can be described as follows:



239 In the case of Th(IV), dimers to hexamers ($2 \leq x \leq 6$) could be identified and corresponding
240 formation constants could be determined because of its single oxidation state in water.⁷⁰ Due to its
241 complex redox chemistry, an extremely large diversity of polynuclear Pu species was observed,
242 including polymers of mixed valence states (Pu(IV) with Pu(III) or Pu(V)).⁷¹ Unfortunately,
243 corresponding formation constants could not be determined. Recent studies suggested that the
244 selected hydrolysis constants of Np(IV) and Pu(IV) by the NEA might be overestimated by
245 approximately one log unit (see e.g. reference 72 and references therein) because they might
246 implicitly include polynuclear Np/Pu(IV) species as well as larger Np/Pu(IV) polymers (small
247 colloids) that are hardly removed from the solution. Nevertheless, only the selected hydrolysis
248 constants of Np(IV) and Pu(IV) by the NEA will be discussed below because recently proposed
249 sets of hydrolysis constants are incomplete and polynuclear species formation constants are
250 missing, which does not allow predicting Np/Pu(IV) solubility.

251 Bilal and Müller³⁷ determined Ce(IV) hydrolysis constants by cyclic voltammetric
252 measurement in aqueous HClO₄ solutions ([Ce]_{tot} = 1.25×10⁻⁴ mol L⁻¹), which are compared with
253 that of Np(IV) and Pu(IV) in Figure 3a. Although a large diversity of polynuclear Ce (including
254 mixed Ce(IV)-Ce(III)) species have been suggested (e.g. Ce(IV)-dimer)⁷⁰, corresponding set of
255 formation constants might be incomplete and questionable.³⁵ Bilal and Müller³⁷ did not account for
256 the formation of polynuclear Ce(IV) species. Cerium(IV) hydrolysis constants might implicitly
257 include such species and, therefore, should be somehow comparable to the selected hydrolysis
258 constants of Np(IV) and Pu(IV) by the NEA. Values of log β_{Ce,1} and log β_{Ce,2} are quite similar to
259 that of Np(IV) and Pu(IV), which supports the idea that these elements can be considered as
260 analogues. However, relatively large deviation is observed for the third and a huge one for the
261 fourth hydrolysis constants: β_{Ce,3} (≈ -1.5) and β_{Ce,4} (≈ -4.4) values are, respectively, 0.8 and 4.4
262 orders of magnitude larger on average than the corresponding constants for Pu (-2.3 and -8.5,
263 respectively). Note that these differences would be larger if Pu(IV) hydrolysis constants were
264 overestimated.⁷² This result is highly contrasting with complexation data with other hard Lewis
265 bases (e.g. OH⁻, F⁻, CO₃²⁻, Cl⁻)⁷³. For instance, formation constants of AnF³⁺_(aq), AnF²⁺_(aq),
266 AnF⁺_{3(aq)} and AnF_{4(aq)} are comparable to those of Ce(IV) (Fig. S1).^{74,75} In fact, Bilal and Müller³⁷
267 determined log β_{Ce,4} less than 0.5 pH unit below the onset of Ce(OH)_{4(am)} precipitation (determined
268 visually). We suspect that log β_{Ce,3} value determined by Bilal and Müller³⁷ might have been
269 affected by the formation of small Ce(IV) colloids, and that log β_{Ce,4} very likely refers to the
270 reaction $Ce^{4+} + 4 OH^- \rightleftharpoons Ce(OH)_{4(am,fresh)}$, where Ce(OH)_{4(am,fresh)} is a freshly precipitated
271 amorphous (colloidal) Ce(IV) hydroxide. The consequence on Ce(IV) and Pu(IV) aqueous
272 speciation is shown in Figure 3b,c ([NaClO₄] = 0.1 mol L⁻¹). Successive Ce(IV) hydrolysis are
273 predicted to occur within a narrow pH-range, and Ce(OH)_{4(aq)} prevails at pH > 3 (Figure 3b). By
274 contrast, Pu(OH)_{4(aq)} prevails only at pH > 6 (Figure 3c).



275
 276 **Figure 3.** (a) Comparison between hydrolysis constants of Np(IV),² Pu(IV),² and Ce(IV).³⁷ Predicted speciation of (b)
 277 Ce(IV) and (c) Pu(IV) versus pH ($[\text{NaClO}_4] = 0.1 \text{ mol L}^{-1}$) using the hydrolysis constants given in Table 1.^{2,37}

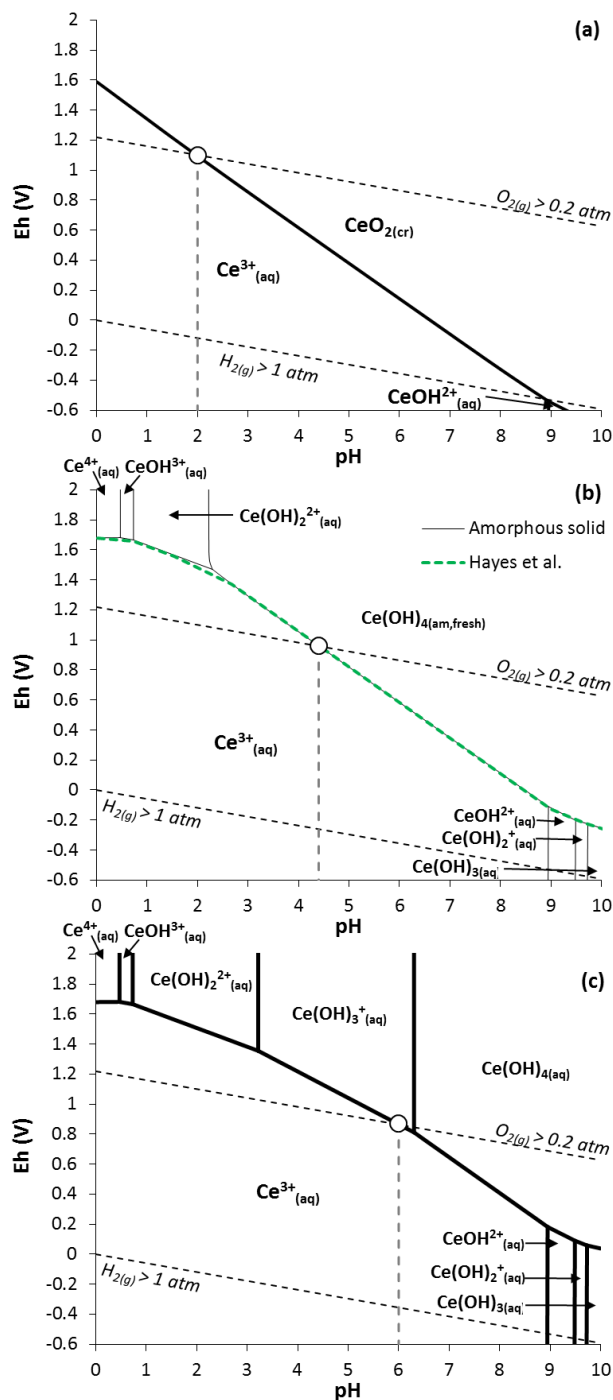
278
 279 **Estimated speciation of Ce**

280 As previously observed for trivalent actinides (Am and Cm) and relevant trivalent
 281 lanthanide analogues (Nd and Eu), the hydrolysis constants are indistinguishable within the given
 282 uncertainties.²⁰ The same should be observed between Ce(IV) and Pu(IV) given their similarities.

283 Because the hydrolysis constants (i) are expected to follow Np(IV) < Ce(IV) < Pu(IV) and (ii) do
 284 not significantly differ between Np(IV) and Pu(IV) given the experimental uncertainties, we
 285 suggest to simply use the complete thermodynamic database of Pu(IV) to estimate Ce(IV) aqueous
 286 speciation. The advantage is that, for further estimations of Ce(IV) behavior in more complex
 287 solutions (e.g. in presence of carbonates² or natural organic matter⁷⁶), the available database of
 288 Pu(IV) can be used for Ce(IV) without any additional corrections. Presently selected hydrolysis
 289 constants for Ce(III) and Ce(IV) are listed in Table 1. Although the Pu(IV) speciation model
 290 provided by the NEA might not be fully mechanistic (polynuclear species are missing, as discussed
 291 above)⁷², it allows predicting overall Pu(IV) solubility quite accurately,^{13,15} which is a sufficient
 292 information for the present purpose. Because the solubility data of Plakhova et al.⁶⁹ at pH < 6 refer
 293 to the half reaction $\text{CeO}_{2(\text{cr,nano})} + 4 \text{H}^+ + \text{e}^- \rightleftharpoons \text{Ce}^{3+} + 2 \text{H}_2\text{O}$, the present estimations have no
 294 consequence on the interpretations of the latter authors, as verified by speciation calculations (not
 295 shown). In particular, the authors found $\log K_{\text{sp}}^0(\text{CeO}_{2(\text{cr,nano})}) = -59.3 \pm 0.3$. This value is higher
 296 than for larger $\text{CeO}_{2(\text{cr})}$ particles, which agree with Schindler equation⁷⁷ and corresponding analysis
 297 of Th(IV) and Pu(IV) data.¹⁵

298 **Table 1.** Comparison between hydrolysis constants of Ce(III) and Ce(IV) used previously^{36,69} and in the present work
 299 (p.w.).

	$\log \beta^{36,69}$	$\log \beta$ (p.w.)
$\text{Ce}^{3+} + \text{H}_2\text{O} \rightleftharpoons \text{CeOH}^{2+} + \text{H}^+$	-8.41 ± 0.08^{78}	-8.41 ± 0.08^{78}
$\text{Ce}^{3+} + 2 \text{H}_2\text{O} \rightleftharpoons \text{Ce}(\text{OH})_2^+ + 2\text{H}^+$	-17.60 ± 0.24^{78}	-17.60 ± 0.24^{78}
$\text{Ce}^{3+} + 3 \text{H}_2\text{O} \rightleftharpoons \text{Ce}(\text{OH})_{3(\text{aq})} + 3\text{H}^+$	-27.23 ± 1.19^{78}	-27.23 ± 1.19^{78}
$\text{Ce}^{4+} + \text{H}_2\text{O} \rightleftharpoons \text{CeOH}^{3+} + \text{H}^+$	0.764^{37}	0.6 ± 0.2^2
$\text{Ce}^{4+} + 2 \text{H}_2\text{O} \rightleftharpoons \text{Ce}(\text{OH})_2^{2+} + 2\text{H}^+$	0.048^{37}	0.6 ± 0.3^2
$\text{Ce}^{4+} + 3 \text{H}_2\text{O} \rightleftharpoons \text{Ce}(\text{OH})_3^+ + 3\text{H}^+$	-1.485^{37}	-2.3 ± 0.4^2
$\text{Ce}^{4+} + 4 \text{H}_2\text{O} \rightleftharpoons \text{Ce}(\text{OH})_{4(\text{aq})} + 4\text{H}^+$	-4.124^{37}	-8.5 ± 0.5^2



300

301 **Figure 4.** pH-Eh diagrams of Ce ($[Ce] = 1.25 \times 10^{-4} \text{ mol L}^{-1}$; $[NaClO_4] = 0.1 \text{ mol L}^{-1}$) assuming (a) formation of $CeO_2(cr)$
 302 ($\log K_{sp}^0 = -64.16$), (b) formation of $Ce(OH)_4(am, fresh)$ ($\log K_{sp}^0 = -56.8$) or (c) no formation of Ce(IV)-(hydr)oxide. In
 303 (b), the pH-Eh diagram calculated by Hayes et al.³⁶ is shown for comparison (only the Ce(IV)/Ce(III) redox
 304 transition is shown). White circles and vertical dotted lines show the pH value corresponding to the Ce(IV)/Ce(III) redox
 305 transition under ambient (air) atmosphere.

306

307 Three different pH-Eh diagrams of Ce are plotted in Figure 4 for $[Ce] = 1.25 \times 10^{-4} \text{ mol L}^{-1}$
308 ($[NaClO_4] = 0.1 \text{ mol L}^{-1}$; corresponding to the experimental conditions of Bilal and Müller³⁷).
309 When assuming the formation of $CeO_{2(cr)}$ (Fig. 4a), for $P_{O_2} = 0.2 \text{ atm}$ ($pH + pe = -\log a_{H^+} - \log$
310 $a_{e^-} = 20.6$), Ce(III) prevails at low $pH < 2$ and rapidly disappears from the solution when pH
311 further increases (not shown; $\log [Ce(IV)]_{aq} = -16.6$ at $pH > 7$ according to our calculations).
312 Although redox conditions may differ from $pH + pe = 20.6$, this result is highly contrasting with
313 previous Ce adsorption studies under ambient (air) conditions, where $\log [Ce]_{aq} > -8$ at $pH = 6$ in
314 $MnO_{2(s)}$ aqueous suspensions, and where little Ce(III) oxidation to Ce(IV) by Fe(III)-(hydr)oxides
315 occurred.²⁹ Hence, $CeO_{2(cr)}$ is very likely not the solubility limiting phase in the latter study. Note
316 that the present pH-Eh diagram (Fig. 4a) agrees very well with previous ones,⁷⁹ although Ce(IV)
317 hydrolysis constants differ, because of the high stability of $CeO_{2(cr)}$.

318 The Ce(IV)/Ce(III) redox transition calculated by Hayes et al.³⁶ is shown as dotted line in
319 Figure 4b. The latter authors used the hydrolysis constants reported by Bilal and Müller,³⁷ which
320 we suspect to account for the precipitation of $Ce(OH)_{4(am, fresh)}$. By using Pu(IV) hydrolysis
321 constants for Ce(IV), we found that both pH-Eh diagrams coincide when $\log K_{sp}^0 \approx -56.8$. This
322 value agrees with $\log K_{sp}^0 = -57.6 \pm 0.7$, which could be estimated for $Ce(OH)_{4(am)}$ using the
323 relationship between $\log K_{sp}^0$ of $An(OH)_{4(am)}$ and An(IV) ionic radii (Fig. 2a). Figure 4c shows the
324 pH-Eh diagram of dissolved Ce. This diagram applies only to Ce aqueous speciation, hence
325 remaining true even when Ce precipitation and/or adsorption to another mineral occur.^{7,80} When
326 $pH + pe = 20.6$, Ce(III) prevails up to $pH \approx 6$. This result is qualitatively consistent with the
327 observation that Ce(III) prevails in solution under ambient conditions in $MnO_{2(s)}$ aqueous
328 suspensions, while Ce(IV) is associated with the solid phase (precipitated or adsorbed onto
329 $MnO_{2(s)}$).^{27,29,39,40} These results further suggest that (i) previously determined hydrolysis

330 constants³⁷ were inaccurate and (ii) Pu(IV) might be a good analogue of Ce(IV).

331

332 **Conclusions**

333 In summary, we briefly reviewed most relevant mechanisms responsible for An(IV)
334 solubility in water and demonstrated the highly consistent behavior of Ce(IV) and An(IV) with
335 quantum chemical calculations, and more specifically the strong resemblance of Ce(IV) aqua ion
336 with the Np(IV) and Pu(IV) aqua ions. Because discrepancies were sometimes observed between
337 experimentally determined thermodynamic parameters of Ce(IV) and An(IV), we chose to simply
338 use the thermodynamic database of Pu(IV) to predict Ce(IV) speciation and solubility. The present
339 estimations are in good agreement with experimental studies of e.g. Ce adsorption to MnO_{2(s)} and
340 Fe(III)-(hydr)oxides. However, the latter comparisons were only qualitative because of the lack of
341 experimental data on redox potentials in MnO_{2(s)} or Fe(III)-(hydr)oxides aqueous
342 suspensions.^{27,29,39} Although, further experimental (e.g. solubility or adsorption) studies are
343 required to verify the present assumptions and to obtain more accurate thermodynamic databases
344 for Ce(IV) and An(IV) (including mono- and polynuclear dissolved species), the present work
345 might yet help (i) to predict more accurately Ce speciation and its fate in environmental conditions
346 (ii) to use more accurately Ce as a proxy of (paleo)redox conditions (iii) to use Ce(IV) as analogue
347 for the study of An(IV) (geo)chemical behavior and (iv) to develop new cerium compounds
348 requiring the control of certain key processing factors.

349 **Acknowledgements**

350 This work has been partially supported by the Agence Nationale de la Recherche through the
351 LABEX CaPPA (ANR-11-LABX-0005-01), as well as by the Ministry of Higher Education and
352 Research, Hauts de France council and European Regional Development Fund (ERDF) through the
353 Contrat de Projets Etat-Region (CPER CLIMIBIO).

354

355 **References**

- 356 1 V. Neck and J. I. Kim, *Radiochim. Acta*, 2000, **88**, 815–822.
357 2 R. Guillaumont, T. Fanghänel, J. Fuger, I. Grenthe, V. Neck, D. A. Palmer and M. H. Rand,
358 *Chemical Thermodynamics, Vol. 5, Update on the Chemical Thermodynamics of Uranium,*
359 *Neptunium, Plutonium, Americium and Technetium*, OECD Nuclear Energy Agency, Data
360 Bank, Elsevier, Amsterdam, 2003.
361 3 G. R. Choppin, *J. Radioanal. Nucl. Chem.*, 2007, **273**, 695–703.
362 4 H. Zänker and C. Hennig, *J. Contam. Hydrol.*, 2014, **157**, 87–105.
363 5 D. W. Efurud, W. Runde, J. C. Banar, D. R. Janecky, J. P. Kaszuba, P. D. Palmer, F. R. Roensch
364 and C. D. Tait, *Environ. Sci. Technol.*, 1998, **32**, 3893–3900.
365 6 T. Fanghänel and V. Neck, *Pure Appl. Chem.*, 2002, **74**, 1895–1907.
366 7 R. Marsac, N. L. Banik, J. Lützenkirchen, R. A. Buda, J. V. Kratz and C. M. Marquardt, *Chem.*
367 *Geol.*, 2015, **400**, 1–10.
368 8 R. Marsac, N. L. Banik, J. Lützenkirchen, C. M. Marquardt, K. Dardenne, D. Schild, J. Rothe,
369 A. Diascorn, T. Kupcik, T. Schäfer and H. Geckeis, *Geochim. Cosmochim. Acta*, 2015, **152**,
370 39–51.
371 9 N. L. Banik, R. Marsac, J. Lützenkirchen, C. M. Marquardt, K. Dardenne, J. Rothe, K. Bender
372 and H. Geckeis, *Geochim. Cosmochim. Acta*, 2017, **215**, 421–431.
373 10 F. Huber, D. Schild, T. Vitova, J. Rothe, R. Kirsch and T. Schäfer, *Geochim. Cosmochim. Acta*,
374 2012, **96**, 154–173.
375 11 X. Gaona, J. Tits, K. Dardenne, X. Liu, J. Rothe, M. A. Denecke, E. Wieland and M. Altmaier,
376 *Radiochim. Acta*, 2012, **100**, 759–770.
377 12 J. Tits, X. Gaona, A. Laube and E. Wieland, *Radiochim. Acta*, 2014, **102**, 385–400.
378 13 V. Neck, M. Altmaier and T. Fanghänel, *Comptes Rendus Chim.*, 2007, **10**, 959–977.
379 14 V. Neck and J. I. Kim, *Radiochim. Acta*, 2001, **89**, 1–16.
380 15 V. Neck, M. Altmaier, A. Seibert, J. I. Yun, C. M. Marquardt and T. Fanghänel, *Radiochim.*
381 *Acta*, 2007, **95**, 193–207.
382 16 V. Neck, R. Müller, M. Bouby, M. Altmaier, J. Rothe, M. A. Denecke and J.-I. Kim, *Radiochim.*
383 *Acta*, 2002, **90**, 485–494.
384 17 V. Neck, J. I. Kim, B. S. Seidel, C. M. Marquardt, K. Dardenne, M. P. Jensen and W. Hauser,
385 *Radiochim. Acta*, 2001, **89**, 439–446.
386 18 V. Neck, M. Altmaier, R. Müller, A. Bauer, T. Fanghänel and J.-I. Kim, *Radiochim. Acta*, 2003,
387 **91**, 253–262.
388 19 M. Altmaier, V. Neck and T. Fanghänel, *Radiochim. Acta*, 2004, **92**, 537–543.

389 20 V. Neck, M. Altmaier, T. Rabung, J. Lützenkirchen and T. Fanghänel, *Pure Appl. Chem.*, 2009,
390 **81**, 1555–1568.

391 21 A. Schnurr, R. Marsac, T. Rabung, J. Lützenkirchen and H. Geckeis, *Geochim. Cosmochim.*
392 *Acta*, 2015, **151**, 192–202.

393 22 Y. Suzuki, T. Nankawa, A. J. Francis and T. Ohnuki, *Radiochim. Acta*, 2010, **98**, 397–402.

394 23 K. B. Krauskopf, *Chem. Geol.*, 1986, **55**, 323–335.

395 24 M. Šulka, L. Cantrel and V. Vallet, *J. Phys. Chem. A*, 2014, **118**, 10073–10080.

396 25 A. Loges, T. Wagner, M. Barth, M. Bau, S. Göb and G. Markl, *Geochim. Cosmochim. Acta*,
397 2012, **86**, 296–317.

398 26 C. R. German and H. Elderfield, *Paleoceanography*, 1990, **5**, 823–833.

399 27 M. Bau, *Geochim. Cosmochim. Acta*, 1999, **63**, 67–77.

400 28 O. Pourret, M. Davranche, G. Gruau and A. Dia, *Chem. Geol.*, 2008, **251**, 120–127.

401 29 A. Ohta and I. Kawabe, *Geochim. Cosmochim. Acta*, 2001, **65**, 695–703.

402 30 J. T. Dahle and Y. Arai, *Int. J. Environ. Res. Public Health*, 2015, **12**, 1253–1278.

403 31 V. K. Ivanov, O. S. Polezhaeva and Y. D. Tret'yakov, *Russ. J. Gen. Chem.*, 2010, **80**, 604–617.

404 32 T. Montini, M. Melchionna, M. Monai and P. Fornasiero, *Chem. Rev.*, 2016, **116**, 5987–6041.

405 33 I. Celardo, J. Z. Pedersen, E. Traversa and L. Ghibelli, *Nanoscale*, 2011, **3**, 1411–1420.

406 34 D. Guyonnet, M. Planchon, A. Rollat, V. Escalon, J. Tuduri, N. Charles, S. Vaxelaire, D. Dubois
407 and H. Fargier, *J. Clean. Prod.*, 2015, **107**, 215–228.

408 35 C. F. Baes and R. S. Mesmer, *The Hydrolysis of Cations*, John Wiley & Sons, New York,
409 London, Sydney, Toronto., 1976.

410 36 S. A. Hayes, P. Yu, T. J. O'Keefe, M. J. O'Keefe and J. O. Stoffer, *J. Electrochem. Soc.*, 2002,
411 **149**, C623–C630.

412 37 B. A. Bilal and E. Müller, *Z. Für Naturforschung A*, 1992, **47**, 974–984.

413 38 L. Al-Attar and Y. Budeir, *Sep. Sci. Technol.*, 2011, **46**, 2313–2321.

414 39 E. H. De Carlo, X.-Y. Wen and M. Irving, *Aquat. Geochem.*, 1997, **3**, 357–389.

415 40 M. Bau and A. Koschinsky, *Geochem. J.*, 2009, **43**, 37–47.

416 41 N. L. Banik, R. Marsac, J. Lützenkirchen, A. Diascorn, K. Bender, C. M. Marquardt and H.
417 Geckeis, *Environ. Sci. Technol.*, 2016, **50**, 2092–2098.

418 42 R. Marsac, N. L. Banik, J. Lützenkirchen, A. Diascorn, K. Bender, C. M. Marquardt and H.
419 Geckeis, *J. Colloid Interface Sci.*, 2017, **485**, 59–64.

420 43 N. L. Banik, V. Vallet, F. Réal, R. M. Belmecheri, B. Schimmelpfennig, J. Rothe, R. Marsac, P.
421 Lindqvist-Reis, C. Walther, M. A. Denecke and C. M. Marquardt, *Dalton Trans.*, 2016, **45**,
422 453–457.

423 44 M. Dolg, H. Stoll and H. Preuss, *J. Chem. Phys.*, 1989, **90**, 1730–1734.

424 45 X. Cao and M. Dolg, *J. Mol. Struct. THEOCHEM*, 2002, **581**, 139–147.

425 46 D. E. Woon and T. H. J. Dunning, *J. Chem. Phys.*, 1994, **100**, 2975–2988.

426 47 T. H. J. Dunning, *J. Chem. Phys.*, 1989, **90**, 1007–1023.

427 48 C. Hättig, A. Hellweg and A. Köhn, *Phys. Chem. Chem. Phys.*, 2006, **8**, 1159–1169.

428 49 C. Hättig, A. Hellweg and A. Köhn, *J. Chem. Phys.*, 2000, **113**, 5154–5161.

429 50 C. Hättig, *Phys. Chem. Chem. Phys.*, 2005, **7**, 59–66.

430 51 F. Weigend, A. Köhn and C. Hättig, *J. Chem. Phys.*, 2002, **116**, 3175–3183.

431 52 A. Klamt and G. Schüürmann, *J. Chem. Soc. Perkin Trans. 2*, 1993, 799–805.

432 53 J. Ho, A. Klamt and M. L. Coote, *J. Phys. Chem. A*, 2010, **114**, 13442–13444.

433 54 R. Ahlrichs, M. Bär, M. Häser, H. Horn and C. Kölmel, *Chem. Phys. Lett.*, 1989, **162**, 165–169.

434 55 *TURBOMOLE V7.1 2016, a development of University of Karlsruhe and Forschungszentrum*
435 *Karlsruhe GmbH, 1989-2007, TURBOMOLE GmbH, since 2007; available from*
436 *http://www.turbomole.com.*

437 56 *AIMAll (Version 17.01.25), Todd A. Keith, TK Gristmill Software, Overland Park KS, USA,*
438 *2017 (aim.tkgristmill.com).*

439 57 *Gaussian 09, Revision A.02, M. J. Frisch et al, Gaussian, Inc., Wallingford CT, 2016., .*

440 58 D. L. Parkhurst and C. A. J. Appelo, *User's guide to PHREEQC (Version 2) : a computer*
441 *program for speciation, batch-reaction, one-dimensional transport, and inverse geochemical*
442 *calculations*, Water-resources Investigation Report 99-4259. USGS, Denver, Colorado, 1999.

443 59 D. Kinniburgh and D. M. Cooper, PhreePlot, <http://www.phreeplot.org>.

444 60 L. Ciavatta, *Ann. Chim.*, 1980, **70**, 551-567.

445 61 G. R. Choppin and E. N. Rizkalla, *Handb. Phys. Chem. Rare Earths*, 1994, **18**, 559-590.

446 62 V. Vallet, P. Macak, U. Wahlgren and I. Grenthe, *Theor. Chem. Acc.*, 2006, **115**, 145-160.

447 63 T. K. Sham, *Phys. Rev. B*, 1989, **40**, 6045-6051.

448 64 H. S. Kim, C. Y. Joung, B. H. Lee, J. Y. Oh, Y. H. Koo and P. Heimgartner, *J. Nucl. Mater.*,
449 **2008**, **378**, 98-104.

450 65 A. K. Tyagi, B. R. Ambekar and M. D. Mathews, *J. Alloys Compd.*, 2002, **337**, 277-281.

451 66 J. Gaillard, L. Venault, R. Calvet, S. Del Confetto, N. Clavier, R. Podor, M. Odorico, J.-L.
452 Pellequer, N. Vigier and P. Moisy, *J. Nucl. Mater.*, 2014, **444**, 359-367.

453 67 X. Beaudoux, M. Virost, T. Chave, G. Leturcq, G. Jouan, L. Venault, P. Moisy and S. I.
454 Nikitenko, *Dalton Trans.*, 2016, **45**, 8802-8815.

455 68 R. H. Schumm, D. D. Wagman, S. M. Bailey, W. H. Evans and V. B. Parker, *Selected values of*
456 *chemical thermodynamic properties [Part 7] Tables for the Lanthanide (Rare Earth) Elements*
457 *(Elements 62-76) in the standard order of arrangement*, National Bureau of Standards, 1973.

458 69 T. V. Plakhova, A. Y. Romanchuk, S. N. Yakunin, T. Dumas, S. Demir, S. Wang, S. G.
459 Minasian, D. K. Shuh, T. Tyliczszak, A. A. Shiryaev, A. V. Egorov, V. K. Ivanov and S. N.
460 Kalmykov, *J. Phys. Chem. C*, 2016, **120**, 22615-22626.

461 70 C. Walther, M. Fuss and S. Büchner, *Radiochim. Acta*, 2008, **96**, 411-425.

462 71 C. Walther, J. Rothe, B. Brendebach, M. Fuss, M. Altmaier, C. M. Marquardt, S. Büchner, H.-R.
463 Cho, J.-I. Yun and A. Seibert, *Radiochim. Acta*, 2009, **97**, 199-207.

464 72 M. Altmaier, X. Gaona and T. Fanghänel, *Chem. Rev.*, 2013, **113**, 901-943.

465 73 R. G. Pearson, *J. Am. Chem. Soc.*, 1963, **85**, 3533-3539.

466 74 R. M. Sawant, N. K. Chaudhuri and S. K. Patil, *J. Radioanal. Nucl. Chem.*, 1990, **143**, 295-306.

467 75 R. M. Sawant, R. K. Rastogi, M. A. Mahajan and N. K. Chaudhuri, *Talanta*, 1996, **43**, 89-94.

468 76 R. Marsac, N. L. Banik, C. M. Marquardt and J. V. Kratz, *Geochim. Cosmochim. Acta*, 2014,
469 **131**, 290-300.

470 77 P. W. Schindler, in *Equilibrium Concepts in Natural Water Systems*, American Chemical
471 Society, 1967, vol. 67, pp. 196-221.

472 78 J. H. Lee and R. H. Byrne, *Geochim. Cosmochim. Acta*, 1992, **56**, 1127-1137.

473 79 P. Yu, S. A. Hayes, T. J. O'Keefe, M. J. O'Keefe and J. O. Stoffer, *J. Electrochem. Soc.*, 2006,
474 **153**, C74-C79.

475 80 M. Kölling, M. Ebert and H. D. Schulz, in *Redox*, eds. D. J. Schüring, P. D. H. D. Schulz, P. D.
476 W. R. Fischer, P. D. J. Böttcher and D. W. H. M. Duijnsveld, Springer Berlin Heidelberg, 2000,
477 pp. 55-63.

478